

Tomography to Visualize Nanoparticle- Assisted Multiphase Flow in Porous Media

Phillip Nwufoh^{*}, Prof. Mi Wang and Prof. Dongsheng Wen

University of Leeds, School of Chemical and Process Engineering, Leeds, LS2 9JT, UK

^{*}Email: pm11pn@leeds.ac.uk

ABSTRACT

In recent years, the use of nanoparticles for enhanced oil recovery has received interest from numerous researchers, however there still are large knowledge gaps to fill in such a vast and developing field. This paper aims to highlight the effect of nanofluids on flow behaviour and oil recovery by the application of electrical resistance tomography as a monitoring tool. Electrical resistance tomography works by producing a distribution of electrical conductivity in the domain of interest, and furthermore various flows can be differentiated on the principle that each fluid has different electrical properties. Although, electrical resistance tomography may not have the spatial resolution of other imaging techniques such as magnetic resonance imaging or computed tomography, it does have the ability to perform reconstructions in real time due to the advent of fast data acquisition systems. Additionally, the use of cross-correlation software allows for the extraction of local velocity and volumetric flow data. This work reports a study on silicon dioxide nanoparticle assisted water-flooding through a number of electrical resistance tomography coupled sand-packed columns. The use of a gravity feed system to introduce pulsations of flooding fluids allows electrical resistance tomography to track local movements of dispersed phase flow signatures in multiphase flows of oil, water, and nanofluid.

Keywords Electrical Tomography, Multiphase Flow, Nanoparticles, Oil Recovery, Tomography

Industrial Application Oil and Gas

1 INTRODUCTION

1.1 Global Energy Trends and Oil Recovery

Global energy consumption is set to increase drastically over the coming decades, with most of this demand being met by fossil fuels. The Environmental Investigation Agency (EIA) released the International Energy Outlook Report in 2017 that suggested world energy consumption would grow by 30% between 2010 and 2040 (International Energy Outlook, 2017). Even though the report highlights the fastest growing energy resources are renewable and nuclear energies (both showing an increase of 2.5% per year), fossil fuels still are predicted to supply around 80% of world energy consumption through to 2040. Therefore, techniques that can improve reservoir characterisation and enhance oil recovery are crucial in finding a solution to the challenge of meeting the ever-growing energy demand. At present the ultimate oil recovery factor for oilfields, on a global scale, is around 35%, meaning that roughly two-thirds of oil that's been discovered is left within the reservoir. This has led to the development of enhanced oil recovery (EOR) techniques that have the potential to recover additional oil left behind.

1.2 Nano-EOR

Certain nanoparticles have characteristics that allow for a reduction in the residual oil saturation during enhanced oil recovery (EOR) operations. These characteristics include i) their ability to travel through the smallest of pore throats due to their minute size (1 – 100 nm) which allows them to penetrate deep into reservoir rocks, ii) their large specific surface area, resulting in an increased contact area of nanoparticles with the oil phase, and better interaction between phases (Singh & Ahmed, 2010), iii) their high multi-functionality allows them to be fabricated for a specific task, thus allowing for nanoparticle characteristics such as particle coatings and morphology to be altered (Kanj et al., 2009;

Ogolo et al., 2009 & Rodriguez et al., 2009) and lastly iv) their ability to change both multiphase and rock-fluid behaviors, allowing for the interfacial tension and wettability of the system to be altered (Hendraningrat & Zhang, 2015; Elsayed 2014; Binshan et al., 2012; El-Diasty, 2015). These key characteristics provide great potential to reduce the residual oil saturation during EOR operations.

1.3 Electrical Tomography

A number of electrical tomography modalities have developed since the late 1980's and have assisted in the applied fields of geophysics, medical engineering, and industrial process systems. Electrical impedance tomography (EIT) works by obtaining an impedance distribution in the domain of interest by using electrodes that induce currents or voltages, and electrodes that measure currents or voltages. A typical EIT sensor consist of a set of equally spaced electrodes mounted across the perimeter of a medium of interest, and represents a non-invasive but intrusive approach as the electrodes must be in contact with the fluids inside the vessel.

EIT has many benefits over other tomographic modalities when considering a flooding setup. It offers an excellent temporal resolution (50 fps), and is therefore effective at capturing changes in flow behavior through time. Other advantages EIT for imaging porous media flow over other modalities include it being practical, and easier to operate. EIT is very easy to setup, and requires minimal training to operate, however data interpretation can be complex. Another important advantage of electrical tomography for imaging porous flows is its ability to perform reconstructions in real time, thanks to the advent of fast data acquisition systems. Thus, electrical tomography can offer online imaging unlike CT and MRI (Rautenbach et al., 2012).

1.4 Aims

This paper reports work conducted with the objective of utilizing electrical resistance tomography (ERT) as a monitoring tool during flooding experiments for enhanced oil recovery. Before the experiments could be conducted a novel sand-pack flooding system had to be developed capable of such requirements. The main goal was to assess the role of nanofluids on oil zones which were bypassed during the water-flooding stage. The main challenge was the limited spatial resolution of ERT which was on the millimeter scale, making it impossible to see the nanoparticles and the pore channels within the sand-pack. However, if ERT is able to capture a large enough zone of residual oil within the sensing zone, then any nano-EOR effects will be easier to see. Additionally, the velocity profiles during the initial period of flooding could provide information on displacement behavior as the initial water front passes.

2 EXPERIMENTAL SETUP

2.1 Sand-pack Flooding System

A new sand-pack flooding system was developed in order to utilise the tomography as a visualisation tool during flooding experiments. The setup involved a sand packed column fitted with dual plane ERT sensors, and pulsation system in which electronically operated solenoid valves allow water and nanofluids to be introduced in timed increments. The flow of fluids through the column was gravity fed, and introduced via drainage bags allowing for a constant pressure head. A vibrating table was incorporated to allow for an evenly and well compacted sand-pack prior to flooding. A new effluent collection system was also developed consisting of an electronically operated rotating table with beakers arranged on top. This allowed for much larger volumes of effluent to be collected automatically. Figure 1 on the following page highlights the system and components.

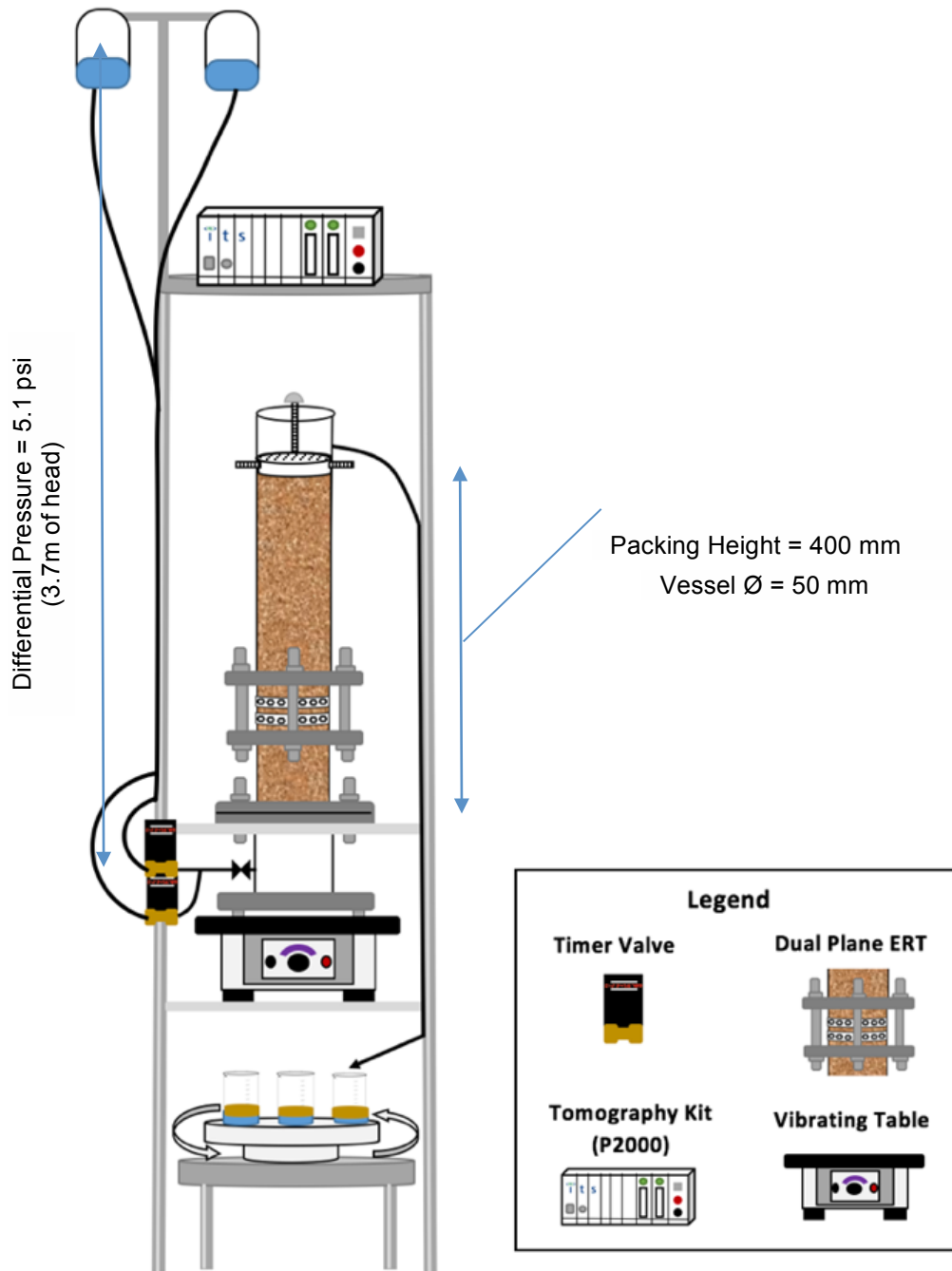


Figure 1 – A Novel ERT coupled sandpack setup with gravity feed system and effluent collection table for analysing cumulative oil recovery. The flow of fluids occurs upwards, from bottom to top.

2.2 Procedure

Firstly, the sand was prepared for the flooding tests by saturating it with known volumes of water and oil. This was done by weighing out a predetermined value of dry sand, and then mixing known volumes of water and oil with the sand. Known volumes of oil (150 ml) and water (50 ml) were then added to the sand, which was subsequently weighed. This provided the saturation content of both water and oil within the sand-pack. The water and nanofluids were then added to the drainage bags. The air in both the water and nanofluid streams needed to be released to avoid the build-up of any backpressure. The packing procedure then began by adding the known volume of oil/water saturated sand into the column, whilst the vibrating table was on. The vibrating table also worked to remove any

bubbles or air that might have been entrapped during the packing process. Next the solenoid timers were set to allow fluids to be introduced to the column automatically in timed increments. Both nanofluid and water were pulsed through the column, each in 5 minute intervals after the initial water flood. The rotation angle and collection times were then set for the rotating effluent collection system. Multiple reference frames were taken using the P2000 tomography kit (ITS, Manchester, UK) during the start of the flooding to achieve the best results. A moving reference was obtained after the initial water front had passed and the system had stabilised, indicated by the levelling out of the local resistivity profiles. The details of the procedures are given below in figure 2.

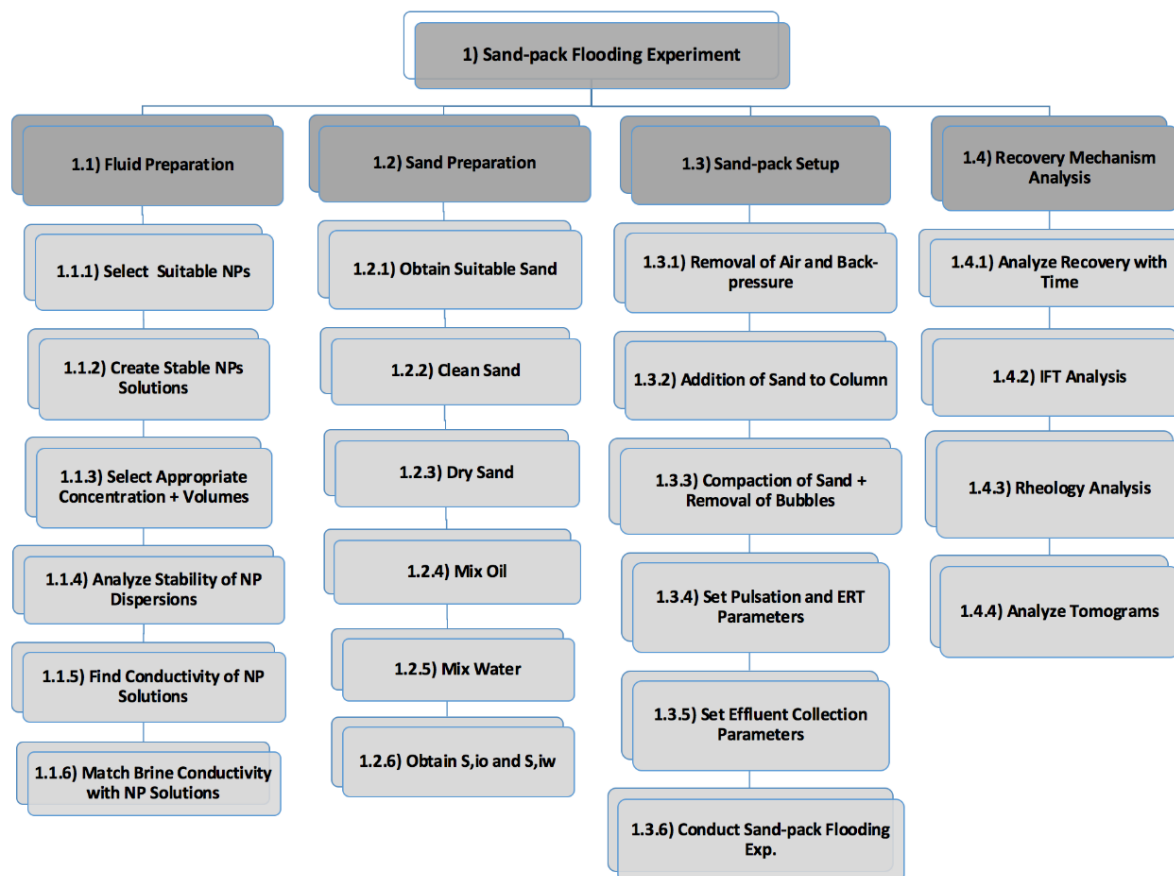


Figure 2 - An overview of the work breakdown including the various steps to be completed during each run.

3 RESULTS

3.1 Flow Imaging

Figure 3 below highlights the ERT visualisations of multiphase flow over the duration of four and half hours, using the linear back projection algorithm. Relative changes of conductivity as a function of time are used to visualise the flow behaviour of oil, water and nanofluid phases as flooding progresses. The tomograms begin with a relatively high concentration of oil phase (blue colour), which is shown to be displaced by the aqueous phase over time. During both runs the concentration of oil was initially seen to deplete from the centre of the column, leaving behind zones of bypassed oil towards the outer perimeter as time progressed.

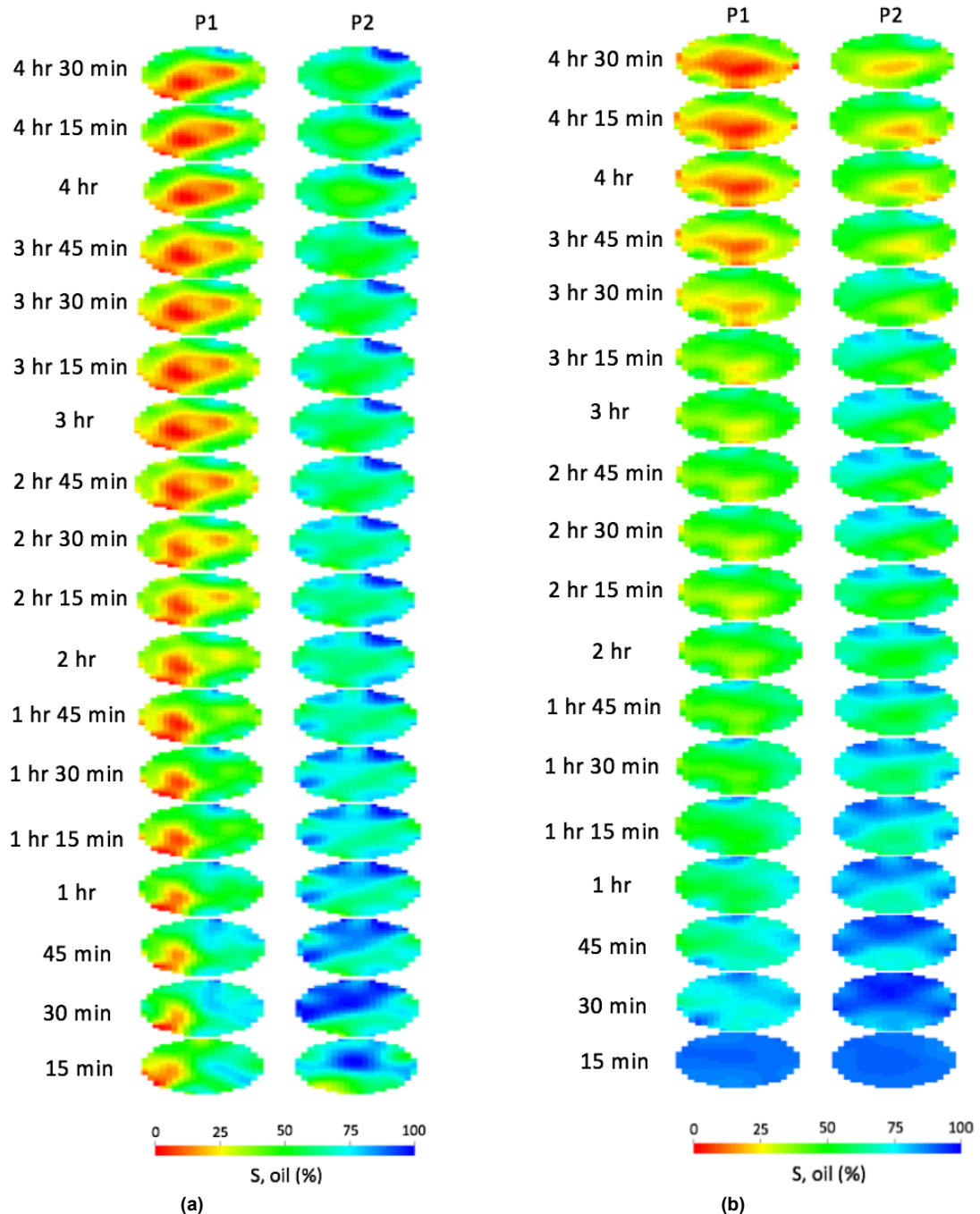


Figure 3 - The tomograms for the flooding runs involving 0.5 wt% SiO₂ (a) and 1 wt% SiO₂ (b) revealing the effect of 10 nanofluid pulsations after 2 hours and 15 mins of water-flooding.

For the flood using 0.5 wt% SiO₂, the first plane P1, initially shows a fingering of both the oil and aqueous phases highlighting clear pathways of flow at the 4 o'clock and 8 o'clock positions (fig 3 (a)). As the flooding progresses the bulk of the oil zone is stripped away and replaced by the laterally spreading aqueous phase (shown in red). A small zone of bypassed residual oil can be spotted at the 1 o'clock position of the tomogram after 2 hours and 15 minutes of water flooding. The introduction of nanofluid can be seen to have a small but noticeable effect on residual oil and consequently flow behaviour. For example, tomograms for P1 shows a residual oil zone at the 1 o'clock position becoming more pronounced, suggesting oil is displaced from beneath the sensing planes and flows up a pathway which feeds into this oil zone. Additionally, a very faint oil zone can also be seen to develop at the 4 o'clock position, which wasn't visible before the introduction of nanoparticles. Plane P2 reveals a larger amount of oil left behind than in P1, which is most likely due to the band of high water saturation (in the 8 o'clock position) that spread laterally as time progressed in P1. Even after the full duration of the experiment the wash out efficiency in plane P2 was still much lower than that of plane P1, and therefore it was assumed that a much larger residual oil zone was left behind in P2. For

example, a relatively high amount of bypassed oil can be seen at the 1 o'clock position. The effect of nanofluids on multiphase flow can clearly be seen in P2 as a zone of oil which accumulates at the 4 o'clock position, approximately 1 hr and 45 mins after introducing ten pulsations nanofluids. This extra oil zone acted as a further evidence to indicate residual oil being released below the sensor and flowing upwards towards the sensing plane.

The tomograms for the run using 1 wt% SiO₂ nanofluids are shown in figure 3(b). The tomograms reveal large residual oil zones at the 1 o'clock and 11 o'clock positions. These particular oil zones were left behind and were left unchanged until the effect of nanofluid took effect approximately 1 hour and 15 minutes after it was introduced. The two residual oil zones swiftly vanish as the flow channels begin to spread laterally and displace additional oil. By the end of the experiment the majority of the oil zones had been displaced, leaving only a very faint zone of bypassed oil left at the 1 o'clock position.

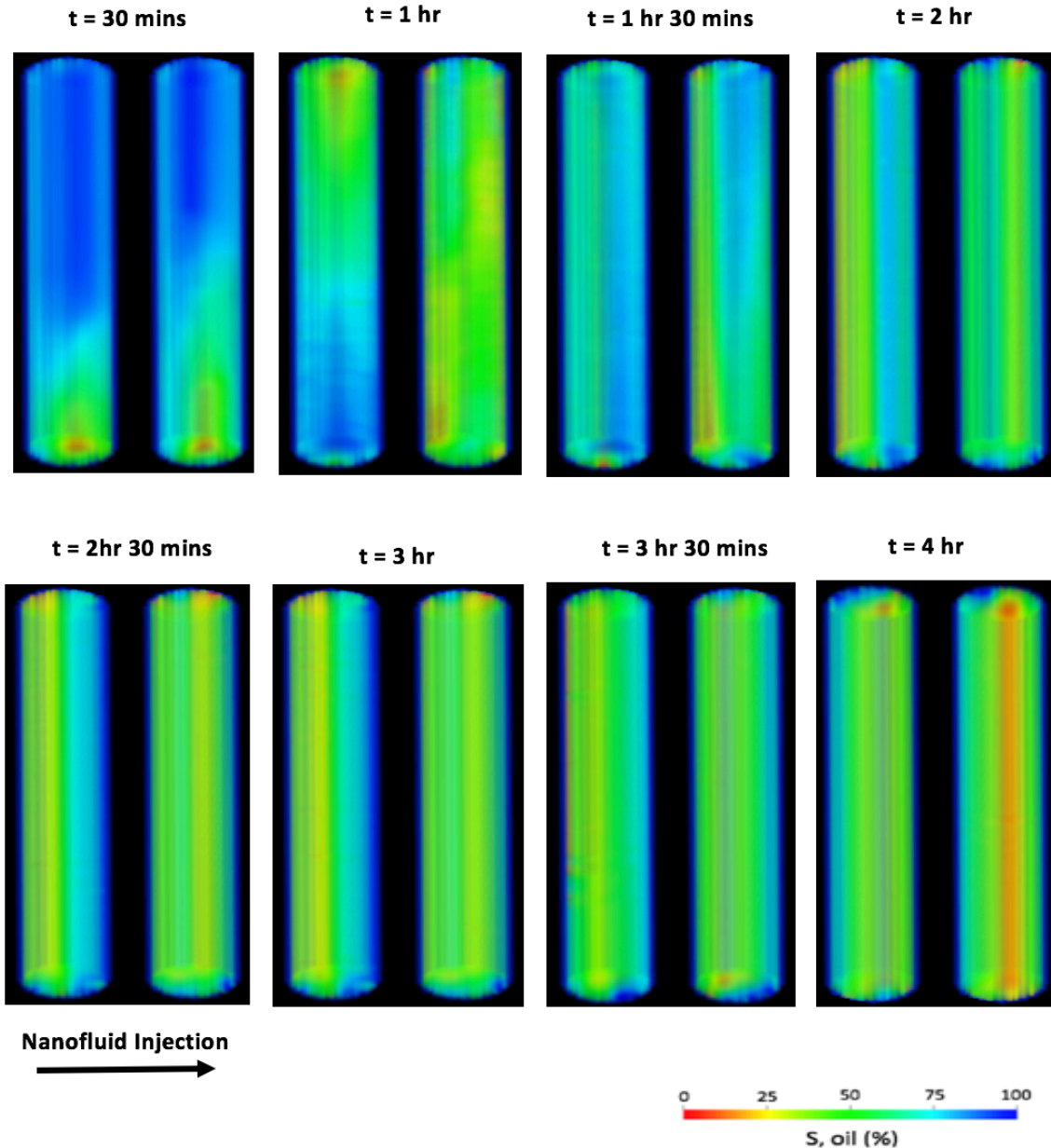


Figure 4 – The volume rendering images produced during the 1 wt% SiO₂ nanofluid run. Each column is composed of 100 stacked images from the same plane, where the columns on the right represent plane P2 and the images on the left are plane P1. The introduction of nanofluids occurred after 2 hrs and 15 mins.

3.2 Volume Rendering

The volume rendering function on the P2+ software allows for different frames of the same sensor plane to be stacked into a 3D image. Figure 4 shows the results of such volume rendering, in which 100 frames were stacked together as a function of time to reveal the displacement behaviour of the flood using 1 wt% SiO₂ nanofluid (fig 4). The first image highlights the initial flooding front showing the predicted piston displacement of the oil phase with a slight preferential flow path on right side of the column. As the flooding progresses a clear zone of residual oil can be seen to develop on the right side of the column after 2 hours. Shortly after the nanofluids were introduced to see their effect, if any, on the bypassed oil zone. As it turns out, the nanofluid had a very noticeable impact in striping away this oil zone, which can be seen on the tomograms as a blue band of oil which becomes less concentrated approximately an hour after nanofluid injection.

3.3 Velocity Profiles

The axial velocity profiles and distributions for both concentrations of SiO₂ nanofluids were generated using the AimFlow software based on the principle of direct cross correlation given as:

$$R_{12}^{(k)}(n) = \sum_{m=1}^k f_1(m) f_2(m+n) \quad (1)$$

Where k is the sample length, n is the offset number and $f_1(m)$ and $f_2(m)$ are the m^{th} up-flow and down-flow respectively.

A sufficient flow signature is needed during multiphase phase flow in order for the cross correlation software to work efficiently. To capture the best flow signatures, the velocity profiles were generated based on the first 30 mins of flooding to ensure there was a sufficient amount of oil present to capture the initial water front. After this time window had exceeded there was a much higher concentration of water around the sensors resulting in a conductivity contrast which wasn't large enough to obtain accurate results.

The results during the 0.5 wt% run are shown in figure 5. Since multiphase flows of oil and water were considered, the velocity distributions also revealed information regarding the displacement behaviour. The areas of lower velocity may be viewed as zones of higher oil concentration because the water phase would be delayed by having to displace the more concentrated zones of highly viscous oil. For example, the velocity distribution shows a valley-like shape of low velocity which are most likely zones of higher oil concentration causing a decrease in the velocity of the aqueous phase. Furthermore, the distributions also paint a picture of a piston-like displacement behaviour, as the zones of higher velocity were found to be quite uniform on one side with lesser fingering effects.

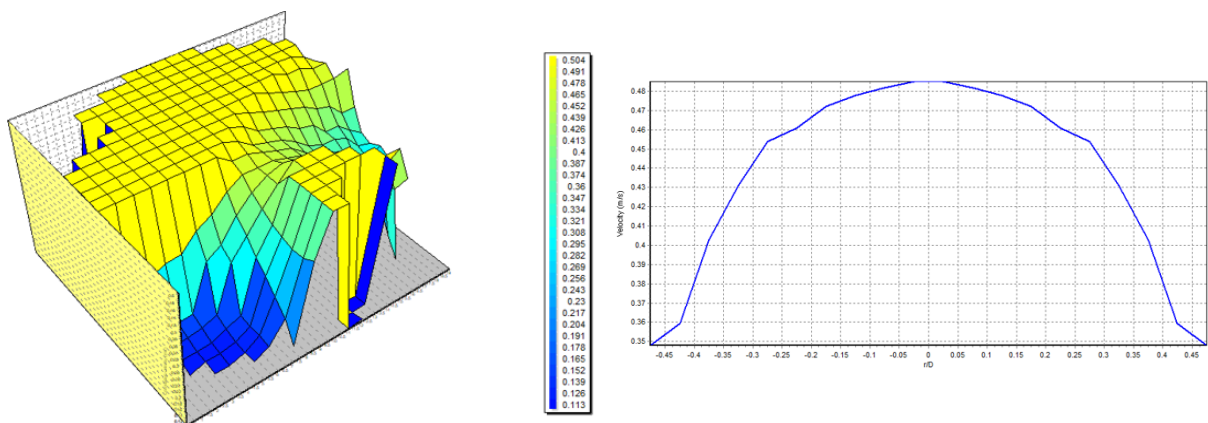


Figure 5 – Velocity distribution (right) and velocity profile (left) from the flood using 0.5 wt% SiO₂ nanoparticles. The data is based on the start of the flood as the initial water front passed and the pursuing 10 mins after.

The distributions for the 1 wt% nanofluid run revealed the velocity to vary more than those obtained during the 0.5 wt% run. However, a very similar flow behaviour can be seen to exist suggesting an

overall piston like displacement as the initial water front passes. The velocity distributions were found to be in agreement with the volume rendering results (fig. 4) which also showed a piston like displacement with a slight preferential flow channel towards one side. The velocity profiles also differ between the two runs, with the profile generated during the 0.5 wt% revealing a more laminar flow with less variations in velocity. For the run with the 1 wt% concentration, a more turbulent flow is seen to develop during the passing of the initial water front resulting in a more varied velocity profile.

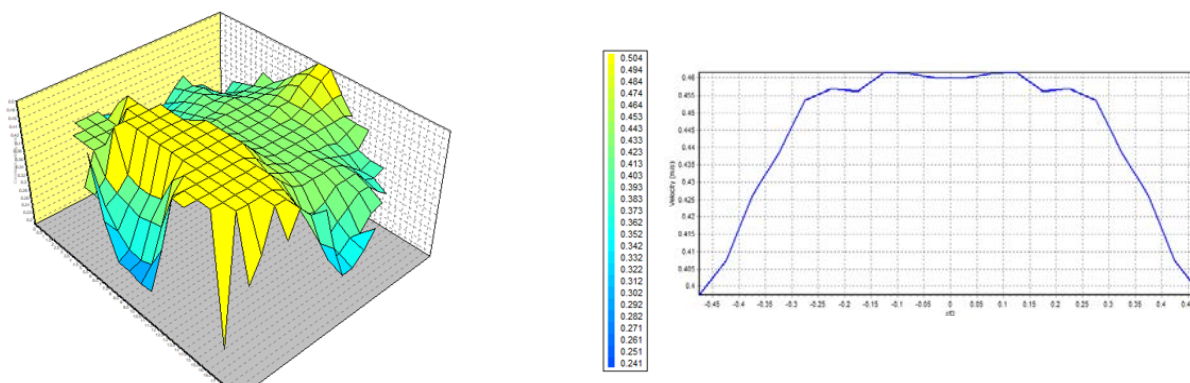


Figure 6 – Velocity distribution (right) and velocity profile (left) from the flood using 1 wt% SiO₂ nanoparticles. The data is based on the start of the flood as the initial water front passed and the pursuing 10 mins after.

4 CONCLUSIONS

A novel sand-pack setup and effluent collection system has been developed during the scope of this research. Tomography (ERT) has been shown to be an effective tool in monitoring multiphase flow behaviour during flooding experiments to investigate oil recovery. The tomograms also crucially reveal the effect of SiO₂ nanofluid on residual oil zones and flow behaviour. The volume rendering function was found to be a good tool in monitoring local residual oil as a function of time, clearly showing zones of depleted oil after the introduction of nanofluids. AimFlow cross correlation software provided velocity distributions of the initial water front and during the first 15 minutes of the experiment, where the flow signatures are large enough to give valid results.

REFERENCES

- EL-DIASTY, ABDELRAHMAN. (2015) The Potential of Nanoparticles to Improve Oil Recovery in Bahariya Formation, Egypt: An Experimental Study, SPE 174599
- ELSAYAD R. ABDEL F. (2014) A Comparative Study between nanoparticles Method and the Other Methods for Increasing Heavy Oil Recovery, MSc. thesis, Suez University
- ENVIRONMENTAL INVESTIGATION AGENCY (2017). *International Energy Outlook 2017*.
- HENDRANIGRAT, L and JULIEN, Z. (2015) Polymeric Nanospheres as A Displacement Fluid in Enhanced Oil Recovery. *Appl Nanosci* 5.8: 1009-1016. Web.
- JU, B., FAN, T. and LI, Z. (2012) Improving water injectivity and enhancing oil recovery by wettability control using nanopowders. *Journal of Petroleum Science and Engineering*, 86-87, pp.206-216.
- KANJ, M., FUNK, J. and AL-YOUSIF, Z. (2009) Nanofluid Coreflood Experiments in the ARAB-D. *SPE*, SPE 126161.
- OGOLO, N., OLAFUYI, O. and ONEYEKONWU, M. (2016) Enhanced Oil Recovery Using Nanoparticles. In: *SPE Saudi Arabia Section Technical Symposium and Exhibition*. SPE International.7

RUAUTENBACH C, MUDDE R.F., YANG X., MELAEEN M.C., HALVORSEN B.M. (2013) A Comparative Study between Electrical Capacitance Tomography and Time-Resolved X-Ray Tomography. *Flow Measurement and Instrumentation* 30: 34-44. Web

RODRIGUEZ E, ROBERTS MR, YU H, HUH C and BRYANT SL. (2009) Enhanced Migration of Surface-Treated Nanoparticles in Sedimentary Rocks. SPE Annual Technical Conference and Exhibition, New Orleans. SPE 124418.

SINGH, S., AHMED, R. (2010) Vital Role of Nanopolymers in Drilling and Stimulations Fluid Applications. Paper SPE 130413 presented at the SPE annual technical conference and exhibition, Florence, Italy

